Enhanced Responsiveness of Cortical Neurons During Sleep

(睡眠時における大脳皮質ニューロン応答性の増強)

2020

筑波大学グローバル教育院

School of Integrative and Global Majors in University of Tsukuba

Ph.D. Program in Human Biology

松本　すみ礼

Sumire Matsumoto

筑波大学

University of Tsukuba

博士　(人間生物学)　学位論文

Ph.D. Dissertation in Human Biology

Enhanced Responsiveness of Cortical Neurons During Sleep

(睡眠時における大脳皮質ニューロン応答性の増強)

2020

筑波大学グローバル教育院

School of Integrative and Global Majors in University of Tsukuba

Ph.D. Program in Human Biology

松本　すみ礼

Sumire Matsumoto

Table of Contents

Abstract

Cortex exhibits large shifts in its activity depending on the vigilance state. Wake and rapid eye movement sleep are characterized by irregular firing of cortical neurons while during slow wave sleep these neurons show synchronous alterations between silent (OFF) period and active (ON) periods, named slow wave activity. The neuronal mechanism underlying these phenomena are not fully understood. By evaluating stimulus-evoked cortical responses, I investigated the cortical network state across sleep-wake cycle. I measured local field potentials and multi-unit activity in the cortex in response to repeated brief optogenetic stimulation of thalamocortical afferents. The responses in both local field potential and multi-unit activity were considerably increased in sleep compared to wake, with larger responses during slow wave sleep than during rapid eye movement sleep. Responses to stimuli were slightly but significantly larger during slow wave sleep-OFF periods than during slow wave sleep-ON periods. The kinetics of multi-unit activity response revealed a possibility that the enhanced cortical responsiveness can be discussed within the context of reduced feed-forward inhibition. Also, I applied long-term single spike sorting to the recording data and successfully obtained satisfactory single spikes throughout 24 h recording. The enhanced responsiveness of cortical network during slow wave sleep could be a key phenomenon in the neuronal mechanism of slow wave activity.

Introduction

Neuronal Activity of Cortex During Sleep

Behaviorally, sleep is characterized by loss of consciousness, increased arousal threshold, and immobility[1]. Despite decreased communication with the periphery during sleep, cortical neurons remain active, although the activity pattern is strikingly different. It switches from ongoing irregular firing during wake to synchronized rhythmic oscillations between silent (OFF) and active (ON) periods[2], [3], called slow wave activity (SWA) in non-rapid eye movement (NREM) sleep or slow wave sleep (SWS). SWA is typically quantified by measuring the spectral power of electroencephalogram (EEG) or local field potential (LFP) in the delta (0.5 ~ 4 Hz) range. The power of SWA reflects the sleep need, the higher delta power will be observed after prolonged wake and it decreases by having sleep[4].

Previous studies have reported the improvement of cortical performance by SWS and SWA, including memory consolidation[5], [6]. Also, the amount of SWA varies between the region of cortex depending on how much the area of the cortex has been used during preceding wake[7], [8]. SWA has been considered to play an important role in cortical function. However, the underlying neuronal mechanisms is not fully understood.

In vitro acute brain slice recordings revealed that slow wave can be observed in the isolated cortical slice[9], suggesting that the slow oscillation can be

potentially generated only by cortical neurons. Also, from *in vivo* study, slow waves has shown to be traveling through cortex[10], indicating that a cortico-cortical communication is involved to the synchronization or propagation of SWA during SWS.

Another proposed neuronal mechanism is the construction of neuronal loops that can generate delta oscillation by cortical, thalamic and reticular neurons that has been revealed by *in vivo* intracellular recording[11]. Regarding the activity of thalamic neurons, slow rhythm in neural activity were also observed in thalamic slices *in vitro*[12]. These studies indicate an active role of thalamic neurons in SWA rhythm generation.

Both or either cortico-cortical and thalamocortical communication might contribute to generate slow rhythm of the neuronal activity, and additional cortico-cortical mechanism to achieve the synchronization among numerous amounts of neurons is expected. The behavior of cortical neurons and its network activity during SWS must be the key component to fully elucidate the SWA mechanism.

Measurement of Evoked Cortical Response

In addition to observations of spontaneous neuronal activity, measurements of evoked cortical responses can be used to probe the functional state of the cortical network during wake and sleep[13]–[20]. Sensory stimuli can reach the cortex during SWS, which allows for studying the effect of sleep-wake

transitions on cortical responsiveness[15], [17]–[19]. Cortical reactivity indeed changes between wake and sleep, but the effect varies dependent on the sensory modality and type of stimulus. In the somatosensory cortex, both response depression and enhancement are observed during sleep compared with wake. In human subjects, sensory evoked potentials are smaller during NREM sleep compared with wake[15]. In macaques, responses to tactile stimuli are significantly decreased during SWS compared with wake[17]. Electrical activation of the medial lemniscus, an ascending bundle in the brain stem that carries sensory information to the thalamus, results in smaller responses in SWS compared with those in the preceding wake episode[20]. On the other hand, whisker deflections in rats produce larger evoked responses, but exhibit faster adaptation to repeated stimuli during SWS compared with wake[18]. Auditory stimulation in rats evokes cortical responses that are comparable across vigilance states[19]. Sensory stimulation or pre-thalamic stimulation involves subcortical structures and do not solely reflect changes in cortical circuits across sleep-wake states. The complexity of the pathway may cause those inconsistencies. Direct activation of cortex or thalamocortical afferents makes it possible to circumvent any effect occurring at pre-thalamic pathways. Electrical stimulation of the visual thalamus in cats shows decreased cortical responses during SWS compared with wake and REM sleep[21]. In human subjects, transcranial magnetic stimulation (TMS) was performed combined with high-density EEG recording[16], [22], [23]. They observed larger evoked cortical response in sleep compared with wake, while the propagation of the evoked activity

beyond the stimulation site was smaller. No definitive explanation for the increased responses was provided so far, due to the limit of the resolution of evoked signals and the neuronal activity underlying this phenomenon is not clear.

I investigated the reaction of the cortical network to repeated, brief optogenetic thalamocortical activations to understand the precise neuronal activity during the response across vigilance states. Cortical LFP and multi-unit activity (MUA), single unit activity (SUA) from primary motor cortex (M1) were measured to capture not only the direct thalamocortical effects, but also the spread of excitation within the cortex in freely behaving mice over prolonged periods of time to ensure consistent delivery of stimuli across many natural sleep-wake transitions.

Materials and Methods

Animals

Experimental procedures were approved and carried out in accordance with local and national regulations following approval by the animal care and use committee of the University of Tsukuba. C57BL/6J male mice aged 13–26 weeks were used for surgery and recorded for about 6 months (mean ± SD age at virus injection: 14.4 ± 1.5 weeks; at implantation of tetrode: 22.4 ± 3.6 weeks; at first recording: 25.8 ± 6.1 weeks, Jackson Laboratory). Mice were housed under a 12 h light/12 h dark cycle with food and water available ad libitum.

Adeno-associated Virus (AAV) Injection

Mice were anesthetized by an intraperitoneal injection of avertin (0.3 ml/kg) and inhalation of isoflurane (4% for induction and 1–2% for maintenance). pAAV10-eF1a-ChR2-mCherry was injected unilaterally into the ventral posteromedial nucleus (VPM) of the thalamus (−1.86 A/P, +1.8 M/L, −3.5 D/V, 140 nl) in the left hemisphere to produce the expression of Channel rhodopsin 2 (ChR2).

Tetrode Implantation

After sufficient recovery from the virus injection (at least 2 weeks), tetrodes were implanted using an electrode manipulator, a so-called microdrive, in addition to an EEG skull screw electrodes and electromyography (EMG) wire electrodes. The mice were anesthetized with avertin and isoflurane as described above, and the skull was exposed through a skin incision. The surface of the brain was exposed by craniotomy. After removing the dura, a microdrive system with 6 tetrodes (KANTHAL Precision Technology, nichrome, 14 μm diameter) was surgically implanted in mice together with two EEG wires (A-M Systems, silver) attached to stainless steel screws, two EMG electrodes in the neck muscle (Cooner wire), and a ground wire (A-M Systems, stainless steel) attached to stainless steel screw and optical fiber. Three tetrodes each were placed in M1 cortex layer 5 of the right and left hemispheres (1.4 A/P, ±2.0 M/L, −1.4 D/V) and one tetrode was placed into the ventral hippocampal commissure (vhc; −0.9 A/P, 0.8 M/L, −2.4 D/V). An optical fiber was implanted into the primary somatosensory cortex (S1) in the left hemisphere (−4.37 A/P, −0.7 M/L, −1.74 D/V, 30°, THORLABS). Mice were single-housed after surgery under a 12 h light/12 h dark cycle with food and water available ad libitum.

Extracellular Recording

After sufficient recovery from microdrive implantation (at least 2 weeks), the mice were habituated to the recording chamber. The chamber has a suspending recording tether with a custom designed pulley system to allow mice to move freely without disturbing their behavior by interference from the tethers, amplifiers, and optical fibers. Data acquisition and online spike detection were performed using 32-ch Digital Lynx 4SX system (Neuralynx). LFP, EEG, and EMG signals were digitized at 1 kHz, after band-pass filtering at 0.1 Hz–10 kHz for LFP, 10–500 Hz for EEG, and 10–1kHz for EMG. LFP were recorded from one electrode of each tetrode with the vhc tetrode as a reference. Units were simultaneously recorded from all four leads of the tetrodes and digitized at 32 kHz after band-pass filtering at 600 Hz–6 kHz. The amplitude threshold for spike detection was manually decided for each tetrode in the range of 50–200 μV.

Optical Stimulation

Optical stimulation was performed using a laser controlled by Master-8 (AMPI) and custom-built TTL generator based on Arduino (Arduino). I used an average of 85.6 mW with about 30% of reduction from the laser to the fiber tip attached to the brain. For the single pulse stimulation, a pulse (duration: 5 ms) was automatically delivered every 5 ± 1 s. The total number of stimuli

delivered during the 24 h recording used in the analysis were mean ± SD in all state: 17264.6 ± 28.9, wake: 7319.9 ± 864.2, SWS: 9053.4 ± 727.9, REM: 891.3 ± 477.0.

Sleep Deprivation

Recordings were started at Zeitgeber time (ZT) = 0 (usually at 9 AM) and mice were sleep-deprived for 4 h from ZT = 0 to ZT = 4 by cage change and gentle handling while optogenetic stimulation was ongoing. After sleep deprivation, mice were freely allowed to enter recovery sleep. As baseline we used recordings from the mice in unperturbed condition one day before and in two animals also one day after the sleep deprivation day. Average response amplitude did not show extreme change between the pre- and post-sleep deprivation control.

Histology

The recording site and ChR2 expression were histologically confirmed after completion of all experiments. Mice were anesthetized with avertin (0.3 ml/kg) or chloroform (10%). First, the tissue near the tip of each tetrode was lesioned by direct current injection (30 μA, 7 s into each tetrode) using a current generator to visualize the recording sites after brain slice preparation.

After current injection, the mice were transcardially perfused with phosphate-buffered saline (approximately 50 ml/mice) and 10% formalin neutral buffer solution (approximately 50 ml/mouse). The microdrives were removed and the brain tissue carefully removed and immersed in 10% formalin neutral buffer solution at 4 °C overnight for fixation. The next day, the brains were placed into 30% sucrose solution for cryoprotection and embedded into O.C.T. compound (Tissue-Tek) at −80 °C for at least 1 h. Brains were sliced by cryostat at 30 ~ 50 μm and mounted on microscopy slides. ChR2 expression was assessed by observing the mCherry signal without any further staining. Nissl staining was performed overnight at 4 °C to reveal the lesioned recording site (NeuroTrace, 1:500). After washing with phosphate-buffered saline, slices were mounted on slides. ZEISS Axio Zoom. V16 (Carl Zeiss Co., Ltd.) and LSM700 (Carl Zeiss Co., Ltd.) microscopes were used for image acquisition.

Data analysis

Data were analyzed using custom-written programs in Matlab (Math Works) and Graph Pad Prism 7 (GraphPad Software). Results were considered significant for p-values < 0.05.

Sleep scoring. Sleep scores were determined using surface EEG signals alone or in combination with LFP and surface EEG signals in combination

with EMG signals with Matlab-based sleep scoring software. Each 4-s epoch was staged into wake, SWS (NREM sleep), and REM sleep. Wake was scored based on low amplitude, fast EEG activity, and high EMG power. SWS was characterized by high delta oscillation and low EMG power. REM sleep was characterized by a theta band-dominated EEG and atonia in the EMG signal.

Single Spike Sorting. Single spike sorting was achieved with Spike Sort 3D software (Neuralynx) offline using tetrode data for a maximum of 1 h. Clusters were considered to represent SUA if the isolation distance was >=20, L-ratio <=0.3[24], [25]. Units with spike wave forms with a peak-to-peak width less than 250 μs were classified as inhibitory neurons, while units with a longer width were classified as excitatory neurons.

Evoked response analysis. The amplitude of an optogenetically evoked LFP was determined from 30 ms time window after each stimulus onset. The 10th to 90th percentile difference in the distribution of samples in this time window of each stimulation was used as the evoked LFP amplitude (Figure 4A). An evoked-MUA response was determined by the number of action potentials within 30 ms of each stimulus presentation after subtracting the basal activity. Basal activity was defined as the sum of spikes in a 300 ms time window before stimulus delivery divided by 10, which is the mean spontaneous activity during 30 ms. For vigilance states the values were normalized to the average in each state over 24 h. For ON/OFF state analysis the values were normalized to the mean of all values across ON and OFF

states. For sleep deprivation experiments, all values were normalized to the mean of the control condition values.

ON/OFF Period Detection. OFF periods just prior to stimulus delivery were detected offline for each tetrode separately, on the basis of LFP characteristics. Large positive deflections of the LFP 10 ms before stimulation compared to the mean of the preceding 3 s were considered OFF state, if the deflection exceeded a threshold based on prior LFP activity. The threshold was set at three times the SD of the gamma power (20–100 Hz) in the three seconds prior to stimulation. This procedure can detect OFF state onsets more rapidly than methods based on delta band filtered data. All other cases were considered ON period stimulations. When multi-unit activity for such classified ON and OFF responses was analyzed, I found a clear reduction in activity just prior to stimulus delivery (Number of units in 10 ms time widow before stimulation per trial (mean ± SD): ON = 0.4 ± 0.3, OFF = 0.2 ± 0.2, N = 43 (tetrodes), $p < 0.01$, paired t-test; Figure 6).

MUA kinetics analysis. Peri-stimulus time histograms in 1-ms bin size calculated from MUA were used for evoked-MUA kinetics analysis. The bin counts of the histogram were divided by the number of traces of each vigilance state and the basal activity (mean of the counts from 200 to 50 ms before the stimulation) was subtracted. Quintiles and Deciles of the response were determined on the basis of the evoked LFP amplitude. The width of the excitation peak was defined as full width of half maximum of the peak in the

histogram. The mode of the MUA distribution evaluated between 10–30 ms after stimulation was considered as peak time of the response. The percentage of inhibition defined as the % of the reduction of unit activity at 50–100 ms after stimulation to the unit activity respect to the same time window before the stimulation.

Analysis of response over 24 h and sleep deprivation. The delta power in SWS was determined as the power in the 0.5–4 Hz range for the 4 s preceding each stimulation time-point. LFP- and MUA- response sizes were first stratified by vigilance states and binned into 1 or 2 h intervals.

Long-term Single Spike Sorting

The MUA data was obtained using 32-ch Digital Lynx 4SX system (Neuralynx) and digitized at 32 kHz after band-pass filtering at 600 Hz–6 kHz. The amplitude threshold for spike detection was decided manually for each tetrode in the range of 50–200 μV. The datapoints in the 1 ms time window of each spikes from all 4 channels of the tetrode were used for spike sorting. The dimension of the data was reduced using principal component analysis to the number of dimension where cumulative contribution ratio is >=90 % in all 4 channels.

Model-based Clustering with a Mixture of Drifting t-distribution (MoDT)[26] was repeatedly applied. After the first application of the sorting algorithm,

the clusters containing more than two single units were visually determined by 3D scatter plotting of peak amplitude of the waveform. The next clustering was applied only to those contaminated clusters to isolate the single units by determining any number of sub clusters. The clustering was conducted repeatedly until obtaining satisfactory clusters.

Results

In vivo Extracellular Recording Combined with Optogenetic Stimulation in Freely Behaving Mice

Thalamic input to the cortex provides a well-characterized pathway for evoking controlled cortical responses [27]–[29]. In this study, AAV containing a plasmid to express ChR2 was injected into the somatosensory thalamus. At the same time, animals were implanted with a multi-tetrode drive system over the ipsi- and contralateral M1 and a light-guide was implanted over S1 (Figure 1A). In rodents, S1 has both anatomic[27] and functional[30]–[34] connections with M1. This recording system therefore allowed us to study synoptically connected networks involving cortical connection from S1 to M1 and M1 to contralateral M1 connections - a mainly monosynaptic excitatory commissure through the corpus callosum. After recovery from surgery and waiting for expression of ChR2 that could evoke clear and stable responses, mice were habituated to the recording chamber and the recording setup. Optogenetic single pulse stimuli (5 ms duration) were delivered at pseudo-random intervals of 5 ± 1 s. These stimuli produced time-locked responses in the LFP recorded by the tetrodes (Figure 1B). Total time spent in wake, in SWS and REM sleep, or in their epoch durations did not differ significantly between stimulation and non-stimulation conditions (Mean ± standard deviation (SD) of time in control versus stimulus conditions [paired t-test],

wake: 12.4 ± 0.9 h versus 10.3 ± 1.7 h [N = 4, p = 0.11], SWS: 10.5 ± 1.1 h versus 12.5 ± 1.4 h [N = 4, p = 0.10], REM: 1.1 ± 1.7 h versus 1.2 ± 0.4 h [N = 4, p = 0.07]). Thus, optogenetic stimulation did not significantly affect the wake sleep pattern.

Enhanced Cortical Responsiveness During Sleep

To compare the stimulation evoked cortical response across vigilance states, the LFP for a total of 300 ms from -50 to +250 ms from the stimulation time point was averaged for each state. Also, the MUA during the same time frame was collected and the histogram of spike time point was described (Figure 2A-D). Vigilance state transition produced rapid changes in the LFP response amplitude accompanied by vigilance state transition, with notably large responses during SWS. On average, SWS LFP responses were several-fold larger compared with wake, while REM responses were still significantly larger compared with wake, but much smaller than SWS responses on both the ipsi- and contralateral sides of the cortical stimulation. These differences in the LFP response amplitude were also reflected in stimulus-evoked MUA. The correlation coefficient between the LFP response amplitude and the MUA response was 0.34 ± 0.04 in wake and 0.75 ± 0.22 in SWS ($p < 0.01$ [48 tetrodes, Pearson's correlation coefficient]).

MUA responses were biphasic in all vigilance states. A brief (30 ms) window with increased unit activity after the optogenetic stimulus was followed by a

longer period of reduced unit activity. To examine whether the balance between rapid increase and following reduction amount of unit activity changes across vigilance states, I defined inhibition as the deficit (number of action potentials missing) below baseline in the 400 ms window following the excitatory phase (30–430 ms post stimulus) and excitation as the number of action potentials above baseline in the 30 ms window immediately following the stimulus. The ratio (inhibition divided by excitation) was 55.5 ± 30.1% for wake, 61.1 ± 39.4% for SWS, and 55.7 ± 30.7% for REM sleep on the ipsilateral and 40.1 ± 21.7% for wake, 49.1 ± 45.7% for SWS, and 68.3 ± 62.8% for REM sleep on the contralateral side. The ratio did not differ significantly between wake and SWS on both the ipsilateral ($p = 0.33$) and contralateral side ($p = 0.12$ [12 tetrodes each, paired t-test]).

In a subset of experiments, I isolated SUA from the MUA response from two mice (Figure 3). On the basis of their waveform, the neurons were classified as 6 putative excitatory and one putative inhibitory neuron on the ipsilateral side and 3 excitatory and one inhibitory neuron on the contralateral side. In all cases, SUA also exhibited increased evoked activity in SWS compared with wake (Figure 2D, $*p < 0.05$, $**p < 0.01$ [paired t-test]).

Neuronal Mechanism of Cortical Responsiveness Variation

While the response size was increased during SWS, I observed a fluctuation of response size even within the same vigilance state. To assess the variation

of response size, the response LFP amplitude and MUA were individually determined at each stimulation. Response LFP amplitude was determined from the fluctuation size in a 30 ms time window after each stimulus onset. (See Materials and methods; Figure 4A, B). An evoked-MUA response was determined by the number of action potentials within 30 ms of each stimulus presentation after subtracting the basal activity. A wide distribution of LFP response amplitudes was observed (Figure 5). These fluctuations in the cortical response during SWS might be linked to ON/OFF oscillations, which are hypothesized to be caused by shifts in excitability[35], [36], and thus the response amplitude. I therefore separated the evoked responses into ON and OFF according to the LFP preceding the optogenetic stimulation (see Materials and Methods; Figure 6). Indeed, spiking activity just before the stimulus onset was significantly lower for OFF responses compared with ON responses, confirming the validity of the LFP-based classification. Surprisingly, evoked LFP responses were slightly, but significantly, larger for OFF responses compared with ON responses, and the evoked unit activity was also higher for OFF responses compared with ON responses (Figure 7). The weak differences between ON/OFF evoked LFP responses did not fully explain the higher responsiveness or wide distribution because the difference in the oscillation did not fully separate large and small responses and both were larger than that during wake. This finding also suggests that OFF periods in the cortex do not prevent the activation of synapses or make it more difficult to evoke action potentials in cortical neurons.

Evaluation of the MUA responses allows for more precise interpretation of the behavior of cortical neurons. A larger MUA response was accompanied by a wider excitation peak, both across vigilance states (Figure 8A) and within SWS (Figure 8B). In SWS, the decile of the response on the basis of the evoked LFP amplitude indicated that a small response occurred in a shorter time window and a larger response occurred in a longer time window (Figure 8C) with a longer time to peak (Figure 8D). In addition, the large excitatory transients were followed by a longer period of inhibition (Figure 8E).

This observation indicates that the overall excitation-inhibition relationship is stable for both small and large responses. The duration of the spiking window in the cortex, however, is largely determined by feedforward inhibition[37] - the wider spiking window of larger SWS responses suggests that feedforward inhibition plays an important role in modulating the evoked cortical responses I observed.

To reduce the number of potential physiological processes that might underlie the vigilance state-dependent fluctuations, I measured the time-course of wake to SWS and SWS to wake transitions. In general, wake to SWS transitions took several minutes to be fully expressed and stabilized thereafter (Figure 9A). Small changes in the response amplitude were observed preceding the behavioral transition, but the largest changes in the response amplitude coincided with the behavioral state transition. Responses grew over 2–3 min afterwards, slightly settled over the next 3 min, and then remained stable for the duration of the SWS episode. SWS to wake transitions were faster (Figure 9B) and showed little adaptation of the response during

the subsequent wake episode. The rapid change in response size and its stability throughout each vigilance state suggesting that the responsiveness change is not caused by continued sleep or wake, but is simply dependent on the vigilance state.

Cortical Responsiveness and Sleep Need

Considerable evidence indicates a vigilance-state dependent modulation of synaptic strength[14], [38]–[40]; the synaptic homeostasis hypothesis postulates that synaptic strength during wake generally and gradually increases with sleep need and is then homeostatically downregulated in subsequent SWS episodes[41], [42]. The synaptic strength modulation may affect the cortical responsiveness change. Thus, according to this hypothesis, the cortical responsiveness might be relevant to homeostatic sleep need regulation.

SWS delta (0.5 ~ 4 Hz) power is the most reliable indicator of sleep need[4]. A well-known oscillation in delta power in the LFP recordings driven by homeostatic sleep need, that peaked at the beginning of the light phase, which is the resting phase for nocturnal animals such as mice, was indeed observed in my recording (Figure 10A). The LFP and MUA responses showed a similar oscillation correlated to light-dark cycle in SWS, while no such oscillation was observed for the wake responses. The median response amplitude every 2 h in each state is shown in Figure 10B. The number of spikes evoked by

optogenetic stimulation also showed this daily fluctuation (Figure 10B). This modulation was also visible in the ratio between the ipsi- and contralateral responses, where the ratio was largest at the beginning of the light phase for both evoked LFP responses and the number of evoked MUA responses (Figure 10C), suggesting that the fluctuation in responsiveness occurred at the connection between left and right M1 through corpus callosum.

I next evaluated the relationship between the response size and delta power of spontaneous LFP signals just before the stimulation in SWS and found only a weak correlation (correlation coefficient ± SD = Ipsilateral LFP: 0.12 ± 0.06, MUA: 0.10 ± 0.06, Contralateral LFP: 0.13 ± 0.06, MUA: 0.12 ± 0.03; $p < 0.01$ [21 tetrodes in each site, Pearson's correlation coefficient], see Materials and Methods).

To distinguish between a coincident circadian effect and a true sleep need dependence, the sleep need was artificially increased by inducing a 4 h sleep deprivation beginning at the start of the light phase. Compared with undisturbed control recording, sleep deprivation produced a significant increase in SWS delta power in the subsequent recovery sleep (Figure 11A), indicating that sleep deprivation indeed increased the sleep need. Optogenetically evoked LFP response amplitudes did not show a sleep need dependent increase over unperturbed control recordings (Figure 11B). Similarly, the MUA response did not differ significantly between these two conditions (Figure 11B). The ratio between the ipsi- and contralateral responses was not affected by the sleep deprivation-induced increase in the sleep need (Figure 11C). Furthermore, the response during forced wake

during 4 h sleep deprivation was averaged every hour to examine if there is an increase in response size accompanied by sleep need accumulation. There was no significant increase (Figure 12). Thus, the cortical responses size fluctuates parallel to the daily sleep need oscillation, but not dependently.

Long-Term Single Spike Sorting

SUA analysis through 24 h recording would provide important insights on sleep homeostasis and cortical activity, yet remains challenging. Spike sorting for long-term data has not been well established. Investigation of SUA is still mostly done with manually sorted short-term recording requiring substantial effort and time. There are several obstacles to long-term recording and spike sorting automation; difficulty of stable long-term recording, drifting of clusters, a high level of background noise. Several algorithms have been proposed in a recent study[43], [44] to solve those problems. To obtain the SUA, I tried several such methods and found out an algorithm that well fit to my recording data, Model-based Clustering with a Mixture of Drifting t-distribution (MoDT)[26]. After first MoDT spike sorting, the clusters were not well separated (Figure 13). By applying the MoDT spike sorting repeatedly (See Materials and Methods), I successively obtained satisfactory clusters (Figure 14). MoDT spike sorting algorithm were applied to18 recording of 24 hours from 4 mice, 53 tetrodes in total. 1~7 single units from each tetrode, 391 clusters in total were isolated. The result of single unit clusters was first

visually verified using the peak amplitude 3D scatter plot of 4 channels of tetrodes every 20 min - 1h with color label of determined single units. Intra-spike interval (ISI) was also calculated to evaluate the quality of clusters, which is typically considered to be a clean single unit if the ISI < 2ms is less than 1% of all ISI[25]. The clusters were considered to be a single unit according to this criterion.

Discussion

I found that cortical LFP and MUA responses were several-fold larger during SWS than during wake, while responses during REM sleep were approximately double the size during wake with vigilance state transitions accompanied by rapid changes in the response amplitude. Larger SWS responses were correlated with longer excitation-time windows but were only slightly affected by ON and OFF periods of slow oscillations. On a longer time-scale, SWS responses exhibited clear daily fluctuation, peaking at the beginning of the rest phase coincident with highest sleep need. The cortical response during recovery sleep after sleep deprivation, however, was not significantly changed.

The increased cortical responses in SWS compared with wake were consistent with findings from TMS in humans[22], [23]. In contrast, sensory evoked responses in humans and animals in natural sleep and under anesthesia typically show smaller and more variable modulation of cortical responses across wake and SWS[15]. For some sensory modalities, no change in cortical responsiveness or even smaller responses in SWS are reported[19]. Sensory evoked responses are typically reduced in REM sleep compared with wake[17]. Recordings of smaller sensory evoked responses in SWS at the thalamic and cortical level support the hypothesis that thalamic filtering significantly contributes to reduced cortical responses[45]. Sensory evoked potentials also

show complex adaptive properties; in rats, the response to whisker stimulation in SWS is large for low frequency stimuli and begins to adapt at more than 5 Hz stimuli in SWS[18]. In the stimulation procedure of my recording, adaptation was not observed because the stimulus, a pulse every 5 ± 1 s was too infrequent for adaptation.

Due to the rapid time-course of the observed changes (Figure 9), it could be speculated that the well-described changes in the neuromodulatory environment between vigilance states contribute to changes in the cortical response amplitude. Wake is characterized by high monoaminergic and cholinergic tone, SWS by low monoaminergic and cholinergic tone, and REM sleep by high cholinergic, but low monoaminergic tone[46]. Acetylcholine (ACh) inhibits principal neurons in layers II to V in the cortex[47] particularly in spiny stellate neurons and their recurrent network[48], [49]. This might be a major contributor to the increased responses in SWS compared with wake. In addition, activation of cholinergic receptors in the piriform cortex inhibits intrinsic connections, but not extrinsic long-range connections[50]. In summary, high cholinergic activity in the cortex suppresses cortical connectivity through both muscarinic and nicotinic receptor activation. Noradrenaline effects on cortical neurons are also inhibitory *in vitro*[51] and *in vivo*[52], and noradrenaline predominantly inhibits sensory cortex neurons. Interestingly, ACh excites thalamic neurons[53] and increases the response reliability of thalamocortical projection neurons[54]. The combination of both these effects shapes the cortical response to sensory-evoked cortical responses

and may explain the discrepancy between sensory evoked stimuli, which involve thalamic circuitry, and direct cortical stimulation, which does not.

Cortical MUA showed clear biphasic responses to optogenetic stimuli. A rapid increase in activity was followed by a more prolonged reduction, which then returned to baseline with or without a rebound. The reduced activity may be caused by a number of factors, such as pre- and postsynaptic inhibition or synaptic fatigue – the data does not allow a differentiation. For the sake of simplicity, I refer to this phenomenon as inhibition. The ratio between the number of unit activity added in the excitatory phase and those missing during inhibition did not change significantly between vigilance states, paralleling prior studies on spontaneous excitation/inhibition balance in wake and SWS[55]. Thalamocortical afferents to somatosensory cortex reliably evoke feedforward inhibition[56] and a reduction in feedforward inhibition leads to a significant broadening of the time window for cortical action potential (AP) generation, illustrating the role of feedforward inhibition in shaping the permissive window for AP generation in cortical circuits[37]. In my results, larger responses in SWS showed a significantly wider time window for spiking. Although it is not possible to definitively differentiate between the contribution of feedforward and feedback inhibition in shaping the inhibitory response on the basis of this experiments, the results are well explained by a decrease in feedforward inhibition contributing to the generation of large cortical responses. Indeed activation of basal forebrain cholinergic input in cortical slices leads to pronounced

disynaptic inhibition[57] by activating non-fast spiking interneurons via nicotinic ACh receptors[47]. A reduction in cortical ACh in SWS is expected to reduce this inhibitory component. The exact circuit cannot be deduced from my data, however, because multiple interneuron types are sensitive to cholinergic modulation.

Thalamocortical synapses show use-dependent depression *in vitro*[58] and *in vivo*[59]. Thus, decreased spontaneous thalamocortical activity in SWS might contribute to the observed increased cortical response. Thalamocortical circuits in SWS, however, exhibit intermittent rhythmic burst firing with peak activity above the persistent activity in wake, and this activity tends to coincide with cortical UP states[60]. The sizes of ON or OFF responses differed only very moderately. In addition, thalamocortical projection neurons are as active in REM sleep as they are in wake - leaving the significant increase in cortical responses in REM sleep unexplained. Thus, purely use-dependent modulation of thalamocortical afferents is an unlikely explanation for the changes I observed.

The responses in SWS were not only significantly larger compared to wake, they also exhibited large trial-to-trial variability. I could rule out ON/OFF fluctuations as a major contributor to this phenomenon, but I currently do not know the mechanisms behind the high variability. The mechanisms underlying ON/OFF transitions in SWS are still not well understood. Fluctuations in excitability due to intrinsic mechanisms such as intracellular

calcium influx triggering Ca^{2+}-dependent K^+ channels or fluctuations in potassium leak channel availability are postulated[35], [36] to underlie the transition to the DOWN state. Alternatively, or in addition, synaptic exhaustion might produce a functional disconnect between cortical neurons and a transition to the DOWN state[61], [62]. The evoked responses were larger in the OFF period compared with the ON period for both the LFP, which mostly reflects synaptic currents, and evoked MUA, which depends on both synaptic input and postsynaptic excitability. Thus, neither the synaptic input to the recorded network nor its reaction to the input in the form of spikes was significantly reduced in the OFF period, indicating that neurons are continuously inhibited and synapses are continuously depressed during the OFF periods. I was unable to determine the precise phase of the OFF period at which stimuli were delivered. It is therefore possible that the mechanisms mentioned above are responsible for triggering transitions, but not for maintaining OFF periods, in accordance with some models of ON/OFF transitions[62].

The small increase in cortical responses in the OFF period can be explained by two mechanisms. First, the amplitude of postsynaptic potentials of cortico-cortical synapses scale with the driving force and are otherwise independent of the ON/OFF period fluctuation[45]. The increased driving force in the OFF state can thus explain the increase in the LFP amplitude. Second, the increased evoked MUA activity may be due to the almost twofold increase in the input resistance in the OFF period compared with the ON period[2], [63].

TMS in humans, time-locked to the phase of slow oscillation, produces larger responses in the UP state compared with the DOWN state[23], [64], whereas sensory evoked potentials show the opposite; thus, the type of input activated seems to influence its impact during ON/OFF oscillations. Early work on the synaptic responsiveness and excitability of cortical neurons[45] showed a decreased synaptic response and propensity to spike. The excitatory response generated by the optogenetic stimulus was short-lived and followed by a significantly longer period of inhibition during SWS; thus, the thalamic input may have re-set the slow oscillation[63]. Interestingly, optogenetic stimulation never produced a stable ON period, indicating that ON period triggering from optogenetic thalamic input is unlikely.

Another possible mechanism of the response size difference is sleep need-dependent control. Within-state analysis of evoked cortical responses revealed a fluctuation within light-dark cycle of the LFP and MUA response size in SWS that paralleled the well-documented oscillation in sleep need. The same fluctuation could not be resolved in wake and sufficient REM data is lacked to analyze it in this manner. According to the synaptic homeostasis hypothesis, cortical synapses are globally strengthened during wake and homeostatically downregulated during SWS[39], [40], and the direction of the fluctuation is compatible with the synaptic homeostasis hypothesis. I therefore also analyzed the response amplitude during wake under sleep deprivation, and found no significant increase (Figure 12). Other mechanisms,

however, such as subtle shifts in the neuromodulatory tone, might also play a role because the correlation between the delta power of preceding spontaneous signals and response size was weak. Indeed, sleep deprivation resulted in a clear increase in recovery sleep delta power, indicating increased sleep need; nevertheless, I did not observe a concomitant increase in the cortical response amplitude. If anything, the response was smaller compared to the baseline recording conditions. There are several possible reasons for this surprising result. The simplest explanation is that response amplitude is modulated by a circadian, but not homeostatic mechanism that happens to follow daily sleep need fluctuations. Alternatively, recovery sleep is characterized by strong slow wave activity; although I did not find a depressant effect of the OFF state on cortical response size, an interaction between strong endogenous slow waves and cortical excitability cannot be ruled out. Indeed, previous work has found a period of refractoriness for electrically evoked cortical responses following strong slow waves[65]. Moreover, sleep need increase after sleep deprivation may engage regulatory mechanisms that are not activated during baseline sleep need fluctuations. It is almost impossible to separate the effects of sleep loss from the effects of sleep deprivation-induced stress. Loss of monoaminergic tone in REM sleep resulted in increased responses; thus, conversely stress-related increases in monoaminergic tone might suppress responses somewhat. Also, the increase in excitatory synaptic transmission observed in SWS is balanced by an upregulation of inhibitory activity. So far, investigations of the synaptic

homeostasis hypothesis have mainly focused on excitatory synapses formed on spines and therefore onto principal neurons. The potential involvement of inhibitory interneurons might have been overlooked.

In this study, a long-term spike sorting was also conducted. The analysis of SUA through long recording may help to further investigate the long-term homeostatic effect in cortical responsiveness. I successfully obtained satisfactory single units by semi-automatic approach utilizing an existing clustering algorithm with repeated application. The verification of sorted single units were visually assessed and also by calculation of ISI. Although the ISI passed the criteria in visually well isolated clusters, some of the low amplitude background noise clusters which should not be treated as single units also showed sufficient ISI indicating the low specificity of unit verification. Therefore, the main verification was visual assessment. As a quantitative cluster verification, two measures have been proposed for the verification of clusters after spike sorting: Isolation distance and L-ratio[66], which I have used during short-time (1 h) spike sorting (see Materials and Methods). I also calculated those measures for long-term data, but it did not fulfil the criteria (typically Isolation distance >=20~25, L-ratio < 0.3[24], [25]) during the entire recording because of the drifting and I therefore did not use as criteria in this long-term spike sorting. Further assessment method for long-term recording must be established to achieve an accurate SUA analysis.

The enhanced, in other words, more synchronized cortical network response might be contributing to achieving the synchronized activity during SWS-SWA. It may also be necessary for maintaining cortical activity in the absence of sufficient peripheral input. Complex circuit mechanisms ensure the arrival of sensory information at the cortex during SWS. The increase in cortical responsiveness in SWS might constitute a safety mechanism in that signals that make it past the thalamic filter generate strong and reliable responses.

References

[1] D. Neckelmann and R. Ursin, “Sleep Stages and EEG Power Spectrum in Relation to Acoustical Stimulus Arousal Threshold in the Rat,” *Sleep*, vol. 16, no. 5, pp. 467–477, 1993.

[2] M. Steriade, I. Timofeev, and F. Grenier, “Natural waking and sleep states: a view from inside neocortical neurons.,” *J. Neurophysiol.*, vol. 85, no. 5, pp. 1969–1985, 2001.

[3] S. Chauvette, S. Crochet, M. Volgushev, and I. Timofeev, “Properties of Slow Oscillation during Slow-Wave Sleep and Anesthesia in Cats,” *J. Neurosci.*, vol. 31, no. 42, pp. 14998–15008, 2011.

[4] X. T. E. Bjorness *et al.*, “An Adenosine-Mediated Glial-Neuronal Circuit for Homeostatic Sleep,” vol. 36, no. 13, pp. 3709–3721, 2016.

[5] R. Stickgold, “Sleep-dependent memory consolidation,” *Nature*, vol. 437, no. 7063, pp. 1272–1278, 2005.

[6] B. Rasch and J. Born, “About sleep’s role in memory,” *Physiol. Rev.*, vol. 93, no. 2, pp. 681–766, 2013.

[7] R. Huber, M. F. Ghilardi, M. Massimini, and G. Tononi, “Local sleep and learning.[see comment],” *Nature*, vol. 430, no. 6995, pp. 78–81, 2004.

[8] R. Huber *et al.*, “Arm immobilization causes cortical plastic changes and locally decreases sleep slow wave activity,” *Nat. Neurosci.*, vol. 9, no. 9, pp. 1169–1176, 2006.

[9] M. V. Sanchez-Vives and D. A. McCormick, “Cellular and network mechanisms of rhytmic recurrent activity in neocortex,” *Nat. Neurosci.*, vol. 3, no. 10, pp. 1027–1034, 2000.

[10] M. Massimini, “The Sleep Slow Oscillation as a Traveling Wave,” *J. Neurosci.*, vol. 24, no. 31, pp. 6862–6870, 2004.

[11] M. Steriade, D. McCormick, and T. Sejnowski, “Thalamocortical oscillations in the sleeping and aroused brain,” *Science (80-.).*, vol. 262, no. 5134, pp. 679–685, 1993.

[12] S. W. Hughes, D. W. Cope, K. L. Blethyn, and V. Crunelli, “Cellular Mechanisms of the Slow (,” *Neuron*, vol. 33, no. 6, pp. 947–958, 2002.

[13] C. Gottesmann, “Neurophysiological support of consciousness during waking and sleep,” *Prog. Neurobiol.*, vol. 59, no. 5, pp. 469–508, 1999.

[14] V. V. Vyazovskiy, C. Cirelli, M. Pfister-Genskow, U. Faraguna, and G. Tononi, “Molecular and electrophysiological evidence for net synaptic potentiation in wake and depression in sleep,” *Nature*, vol. 11, no. 2, 2008.

[15] M. Massimini, M. Rosanova, and M. Mariotti, “EEG Slow (~1 Hz) Waves Are Associated With Nonstationarity of Thalamo-Cortical Sensory Processing in the Sleeping Human,” *J. Neurophysiol.*, vol. 89, no. 3, pp. 1205–1213, 2006.

[16] M. Massimini, F. Ferrarelli, S. Sarasso, and G. Tononi, “Cortical mechanisms of loss of consciousness: Insight from TMS/EEG studies,” *Arch. Ital. Biol.*, vol. 150, no. 2–3, pp. 44–55, 2012.

[17] G. Gucer, “The Effect of Sleep Upon the Transmission of Afferent

Activity in the Somatic Afferent System," *Exp. Brain Res.*, vol. 298, no. 1, pp. 287–298, 1979.

[18] M. A. Castro-Alamancos, "Absence of rapid sensory adaptation in neocortex during information processing states.," *Neuron*, vol. 41, no. 3, pp. 455–64, 2004.

[19] Y. Nir, V. V Vyazovskiy, C. Cirelli, M. I. Banks, and G. Tononi, "Auditory responses and stimulus-specific adaptation in rat auditory cortex are preserved across NREM and REM sleep," *Cereb. Cortex*, vol. 25, no. 5, pp. 1362–1378, 2015.

[20] S. Chauvette, J. Seigneur, and I. Timofeev, "Sleep Oscillations in the Thalamocortical System Induce Long-Term Neuronal Plasticity," *Neuron*, vol. 75, no. 6, pp. 1105–1113, 2012.

[21] M. Palestini, M. Pisano, G. Rosadini, and G. F. Rossi, "Visual cortical responses evoked by stimulating lateral geniculate body and optic radiations in awake and sleeping cats," *Exp. Neurol.*, vol. 9, no. 1, pp. 17–30, Jan. 1964.

[22] M. Massimini, F. Ferrarelli, R. Huber, S. K. Esser, H. Singh, and G. Tononi, "Breakdown of cortical effective connectivity during sleep," *Science (80-.).*, vol. 309, no. 5744, pp. 2228–2232, 2005.

[23] T. O. Bergmann *et al.*, "EEG-Guided Transcranial Magnetic Stimulation Reveals Rapid Shifts in Motor Cortical Excitability during the Human Sleep Slow Oscillation," *J. Neurosci.*, vol. 32, no. 1, pp. 243–253, 2012.

[24] S. J. Middleton and T. J. McHugh, "Silencing CA3 disrupts temporal

coding in the CA1 ensemble," *Nat. Neurosci.*, vol. 19, no. 7, pp. 945–951, 2016.

[25] A. K. Dhawale, R. Poddar, S. B. E. Wolff, V. A. Normand, E. Kopelowitz, and B. P. Ölveczky, "Automated long-Term recording and analysis of neural activity in behaving animals," *Elife*, vol. 6, pp. 1–40, 2017.

[26] K. Q. Shan, E. V. Lubenov, and A. G. Siapas, "Model-based spike sorting with a mixture of drifting t-distributions," *J. Neurosci. Methods*, vol. 288, pp. 82–98, 2017.

[27] R. Aronoff, F. Matyas, C. Mateo, C. Ciron, B. Schneider, and C. C. H. Petersen, "Long-range connectivity of mouse primary somatosensory barrel cortex," *Eur. J. Neurosci.*, vol. 31, no. 12, pp. 2221–2233, 2010.

[28] T. Yamashita and C. C. H. Petersen, "Target-specific membrane potential dynamics of neocortical projection neurons during goal-directed behavior," *Elife*, vol. 5, no. JUN2016, pp. 1–11, 2016.

[29] S. Manita *et al.*, "A Top-Down Cortical Circuit for Accurate Sensory Perception," *Neuron*, vol. 86, no. 5, pp. 1304–1316, 2015.

[30] R. A. Ferenc Matyas, Varun Sreenivasan, Fred Marbach, Catherine Wacongne, Boglarka Barsy, Celine Mateo and C. C. H. Petersen, "Motor Control by Sensory Cortex," *Science (80-.).*, vol. 330, no. November, pp. 1240–1244, 2010.

[31] I. Ferezou, F. Haiss, L. J. Gentet, R. Aronoff, B. Weber, and C. C. H. Petersen, "Spatiotemporal Dynamics of Cortical Sensorimotor Integration in Behaving Mice," *Neuron*, vol. 56, no. 5, pp. 907–923,

2007.

[32] T. Mao, D. Kusefoglu, B. M. Hooks, D. Huber, L. Petreanu, and K. Svoboda, “Long-Range Neuronal Circuits Underlying the Interaction between Sensory and Motor Cortex,” *Neuron*, vol. 72, no. 1, pp. 111–123, 2011.

[33] T. Yamashita, A. Pala, L. Pedrido, Y. Kremer, E. Welker, and C. C. H. Petersen, “Membrane potential dynamics of neocortical projection neurons driving target-specific signals,” *Neuron*, vol. 80, no. 6, pp. 1477–1490, 2013.

[34] J. L. Chen, S. Carta, J. Soldado-Magraner, B. L. Schneider, and F. Helmchen, “Behaviour-dependent recruitment of long-range projection neurons in somatosensory cortex,” *Nature*, vol. 499, no. 7458, pp. 336–340, 2013.

[35] F. Tatsuki *et al.*, “Involvement of Ca2+-Dependent Hyperpolarization in Sleep Duration in Mammals,” *Neuron*, vol. 90, no. 1, pp. 70–85, 2016.

[36] K. Yoshida, S. Shi, M. Ukai-Tadenuma, H. Fujishima, R. Ohno, and H. R. Ueda, “Leak potassium channels regulate sleep duration,” *Proc. Natl. Acad. Sci.*, vol. 115, no. 40, pp. E9459–E9468, 2018.

[37] F. Pouille and M. Scanziani, “Enforcement of Temporal Fidelity in Pyramidal Cells by Somatic Feed-Forward Inhibition,” *Science (80-.).*, vol. 293, no. 5532, pp. 1159–1163, Aug. 2001.

[38] S. Maret, U. Faraguna, A. B. Nelson, C. Cirelli, and G. Tononi, “Sleep and waking modulate spine turnover in the adolescent mouse cortex,”

Nat. Neurosci., vol. 14, no. 11, pp. 1418–1420, 2011.

[39] L. De Vivo *et al.*, "Ultrastructural Evidence for Synaptic Scaling Across the Wake/ sleep Cycle HHS Public Access," *Science (80-.).*, vol. 355, no. 6324, pp. 507–510, 2017.

[40] G. H. Diering, R. S. Nirujogi, R. H. Roth, P. F. Worley, A. Pandey, and R. L. Huganir, "Homer1a drives homeostatic scaling-down of excitatory synapses during sleep," *Science (80-.).*, vol. 515, no. February, pp. 511–515, 2017.

[41] G. Tononi and C. Cirelli, "Sleep and synaptic homeostasis: A hypothesis," *Brain Res. Bull.*, vol. 62, no. 2, pp. 143–150, 2003.

[42] G. Tononi and C. Cirelli, "Sleep function and synaptic homeostasis," *Sleep Med. Rev.*, vol. 10, no. 1, pp. 49–62, 2006.

[43] J. E. Chung *et al.*, "A Fully Automated Approach to Spike Sorting," *Neuron*, vol. 95, no. 6, pp. 1381-1394.e6, 2017.

[44] S. Wiseman *et al.*, "Automated long-Term recording and analysis of neural activity in behaving animals," *Elife*, vol. 6, no. 1, pp. 1–40, 2017.

[45] I. Timofeev, D. Contreras, and M. Steriade, "Synaptic responsiveness of cortical and thalamic neurones during various phases of slow sleep oscillation in cat," *J. Physiol.*, vol. 494, no. 1, pp. 265–278, 1996.

[46] S. H. Lee and Y. Dan, "Neuromodulation of Brain States," *Neuron*, vol. 76, no. 1. Elsevier Inc., pp. 209–222, 2012.

[47] A. T. Gulledge, S. B. Park, Y. Kawaguchi, and G. J. Stuart, "Heterogeneity of Phasic Cholinergic Signaling in Neocortical

Neurons," *J. Neurophysiol.*, vol. 97, no. 3, pp. 2215–2229, 2007.

[48] Eggermann and Feldmeyer, "Cholinergic filtering in the recurrent excitatory microcircuit of cortical layer 4," *Proc. Natl. Acad. Sci.*, vol. 106, no. 28, pp. 11753–11758, 2009.

[49] R. Dasgupta, F. Seibt, and M. Beierlein, "Synaptic release of acetylcholine rapidly suppresses cortical activity by recruiting muscarinic receptors in layer 4," *J. Neurosci.*, vol. 38, no. 23, pp. 5338–5350, 2018.

[50] E. Barkai and M. H. Hasselmo, "Acetylcholine and associative memory in the piriform cortex," *Mol. Neurobiol.*, vol. 15, no. 1, pp. 17–29, 1997.

[51] D. A. McCormick, "Cholinergic and noradrenergic modulation of thalamocortical processing," *Trends Neurosci.*, vol. 12, no. 6, pp. 215–221, 1989.

[52] Y. Manunta and J.-M. Edeline, "Effects of Noradrenaline on Frequency Tuning of Rat Auditory Cortex Neurons," *Eur. J. Neurosci.*, vol. 9, no. 4, pp. 833–847, 1997.

[53] P. Andersen and D. R. Curtis, "The Excitation of Thalamic Neurones by Acetylcholine," *Acta Physiol. Scand.*, vol. 61, no. 1–2, pp. 85–99, 1964.

[54] M. Goard and Y. Dan, "Basal forebrain activation enhances cortical coding of natural scenes," *Nat. Neurosci.*, vol. 12, no. 11, pp. 1444–1449, 2009.

[55] M. Rudolph, M. Pospischil, I. Timofeev, and A. Destexhe, "Inhibition Determines Membrane Potential Dynamics and Controls Action

Potential Generation in Awake and Sleeping Cat Cortex," *J. Neurosci.*, vol. 27, no. 20, pp. 5280–5290, 2007.

[56] L. Gabernet, S. P. Jadhav, D. E. Feldman, M. Carandini, and M. Scanziani, "Somatosensory integration controlled by dynamic thalamocortical feed-forward inhibition," *Neuron*, vol. 48, no. 2, pp. 315–327, 2005.

[57] S. Arroyo, C. Bennett, D. Aziz, S. P. Brown, and S. Hestrin, "Prolonged Disynaptic Inhibition in the Cortex Mediated by Slow, Non- 7 Nicotinic Excitation of a Specific Subset of Cortical Interneurons," *J. Neurosci.*, vol. 32, no. 11, pp. 3859–3864, 2012.

[58] M. Beierlein and B. W. Connors, "Short-Term Dynamics of Thalamocortical and Intracortical Synapses Onto Layer 6 Neurons in Neocortex," *J. Neurophysiol.*, vol. 88, no. 4, pp. 1924–1932, 2017.

[59] S. Chung, X. Li, and S. B. Nelson, "Short-term depression at thalamocortical synapses contributes to rapid adaptation of cortical sensory responses in vivo," *Neuron*, vol. 34, no. 3, pp. 437–446, 2002.

[60] M. Steriade, "Synchronized activities of coupled oscillators in the cerebral cortex and thalamus at different levels of vigilance [published erratum appears in Cereb Cortex 1997 Dec;7(8):779]," *Cereb. Cortex*, vol. 7, no. 6, pp. 583–604, 1997.

[61] M. Bazhenov, I. Timofeev, M. Steriade, and T. J. Sejnowski, "Model of thalamocortical slow-wave sleep oscillations and transitions to activated States.," *J. Neurosci.*, vol. 22, no. 19, pp. 8691–8704, 2002.

[62] C. J. Wilson, "Up and down states," vol. 71, no. 2, pp. 233–236, 2008.

[63] D. Contreras, I. Timofeev, and M. Steriade, “Mechanisms of long-lasting hyperpolarizations underlying slow sleep oscillations in cat corticothalamic networks,” *J. Physiol.*, vol. 494, no. 1, pp. 251–264, 1996.

[64] M. Mukovski, S. Chauvette, I. Timofeev, and M. Volgushev, “Detection of active and silent states in neocortical neurons from the field potential signal during slow-wave sleep,” *Cereb. Cortex*, vol. 17, no. 2, pp. 400–414, 2007.

[65] V. V Vyazovskiy, U. Faraguna, C. Cirelli, and G. Tononi, “Triggering slow waves during NREM sleep in the rat by intracortical electrical stimulation : Effects of sleep / wake history and background activity,” *J. Neurophysiol.*, vol. 101, pp. 1921–1931, 2009.

[66] N. Schmitzer-Torbert, J. Jackson, D. Henze, K. Harris, and A. D. Redish, “Quantitative measures of cluster quality for use in extracellular recordings,” *Neuroscience*, vol. 131, no. 1, pp. 1–11, 2005.

Acknowledgment

I would like to express my deepest gratitude to my supervisor, Dr. Kaspar Vogt, International Institute for Integrative Sleep Medicine (IIIS), University of Tsukuba, for the great supervision and all his supports throughout my Ph.D. course. This dissertation would not be possible without the generous help from him.

I also would like to express my great appreciation for Dr. Robert Greene, UT Southwestern Medical Center, USA, and Dr. Masashi Yanagisawa, IIIS, University of Tsukuba, for their support and advice on this work.

I am also grateful to Dr. Tetsuya Sakurai, my co-academic advisor, and Dr. Keiichi Morikuni, faculty of Engineering, Information and Systems, University of Tsukuba, for providing me an opportunity to join their group as research rotation and to study computational techniques. The long-term spike sorting is a collaboration work with them. I am also grateful to my international co-academic advisor, Dr. Patrick Fuller for his kind support and feedback on this work. I also would like to thank Dr. Vladyslav Vyazovskiy, University of Oxford, for providing me an opportunity to join his group as international research rotation and learn their research techniques, and all his lab members for their kind support during the research rotation.

I would like to acknowledge my thesis committee, Dr. Takeshi Sakurai and Dr. Hiromi Yanagisawa for their insightful comments and encouragement.

I am also very grateful to all the laboratory members, IIIS members for their support and sharing protocols, reagents, and so on, all the faculty members of Human Biology Program and staff at the SIGMA office for the support during these five years in this program.

Last but not least, I want to thank my friends who gave me generous support during my Ph.D. course, and all my family members for the continuous support they have given me throughout my time in graduate school.

Figures

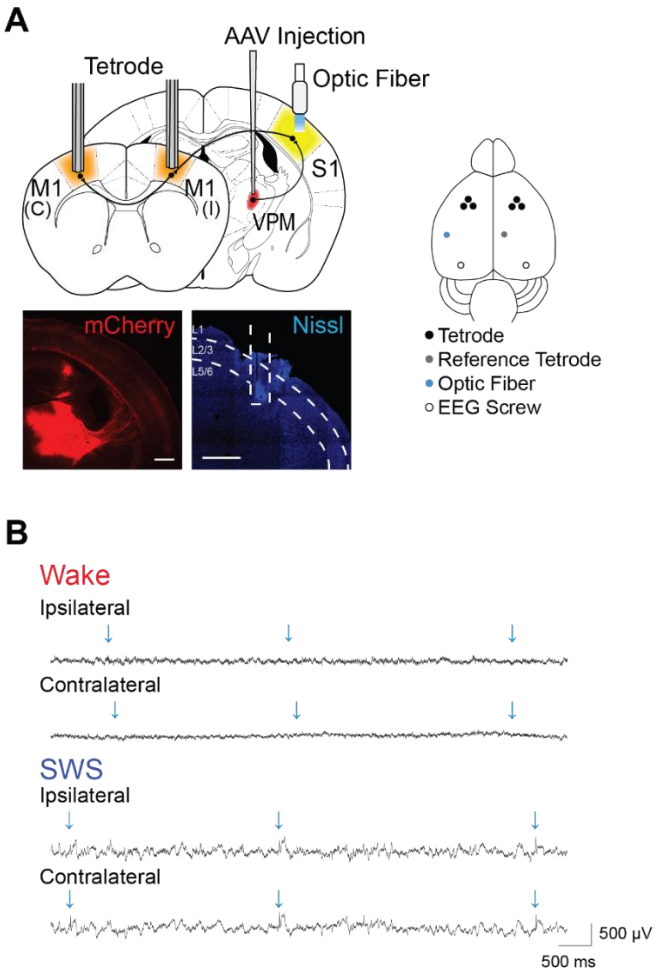

Figure 1. In vivo Extracellular Recording Combined with Optogenetic Stimulation in Freely Behaving Mice

(A) Schematic of virus injection, and placement of optogenetic stimulation and tetrode recordings. AAV-ChR2-mCherry was injected into VPM, an optic fiber was implanted in S1, and three tetrodes were implanted in M1 of each hemisphere. Coronal sections of forebrain stained against mCherry (red) showing the thalamic injection and cortical innervation, and a detailed

coronal cortical section (blue) showing the electrode track. Scale bars: 500 µm. (B) Examples of LFP signals with 5 ms optical stimulation every 5 ± 1 s during wake and SWS. Blue arrows: stimulation time-point.

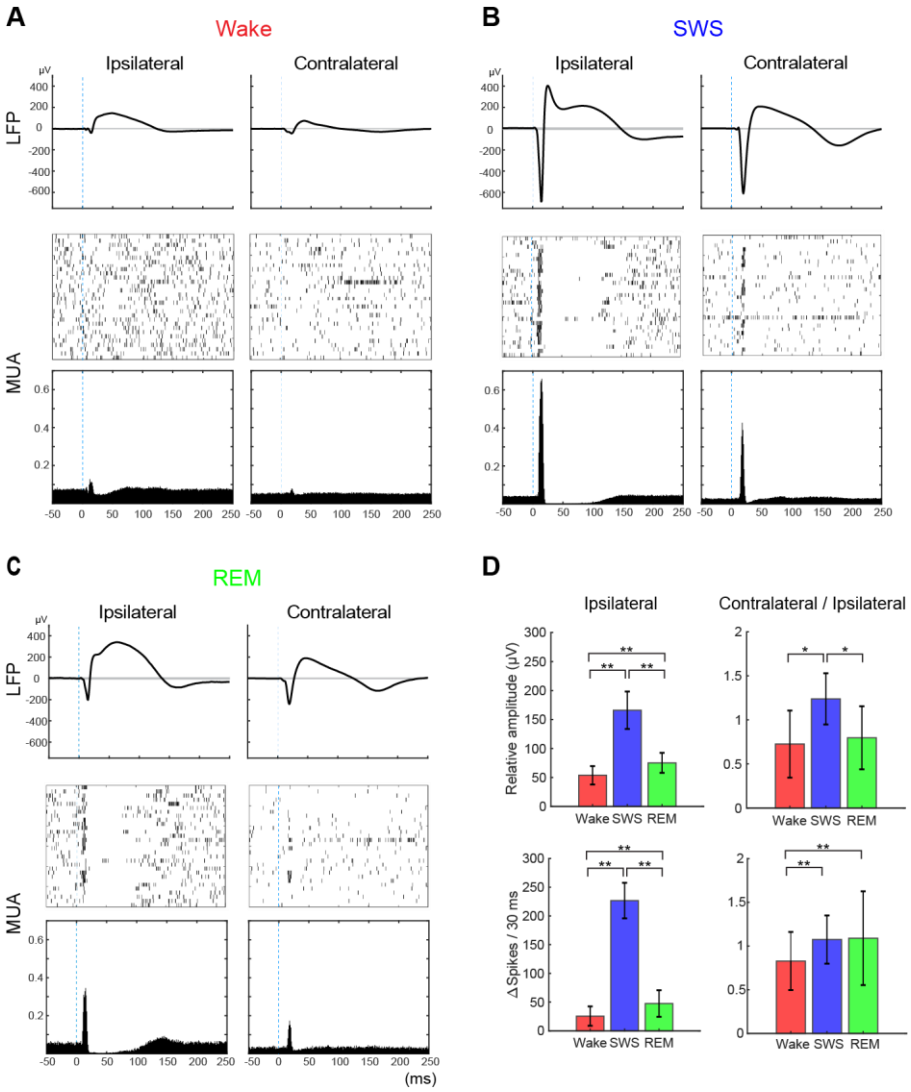

Figure 2. Cortical Responsiveness Across Vigilance State

(A-C) Example of averaged time-locked LFP signals and MUA in each vigilance state. For LFPs, signals from −50 ms before to 250 ms after stimulation were extracted and averaged (gray line: mean ± 3 SD of pre-stimuli LFP signals, top). For MUA, the time-points of unit activity were extracted in the same time windows as for the LFP. Examples of 30 stimulations are shown as a raster plot (middle). Peri-stimulus time

histograms (1-ms bin size) were calculated from the MUA data (bottom). Both LFP- and MUA-responses were larger during sleep compared with wake. (D) Summary of response sizes for both LFP relative to the mean across states (left top) and MUA relative to the mean across states (left bottom, 4 animals, 12 tetrodes from ipsilateral to the activated thalamic input, 12 tetrodes from contralateral). Intracortical response (right two panel) was calculated as the average LFP and MUA response sizes of the three contralateral tetrodes divided by the average of the ipsilateral tetrodes for each stimulus (error bar: SD, *$p < 0.05$, **$p < 0.01$ [12 tetrodes, paired t-test]). MUA were calculated as the number of spikes within 30 ms after stimulation minus baseline activity.

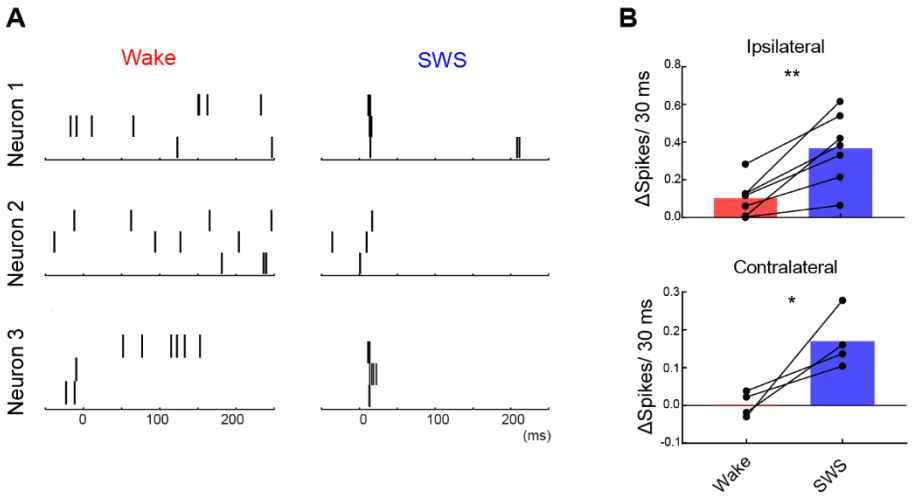

Figure 3. Cortical Response in SUA

(A) Example raster plot of three single units following three stimulations (Neuron 1 and 2 are from ipsilateral, Neuron 3 is from contralateral tetrode). In SWS, single neurons reliably responded to the stimulation. (B) Changes of SUA across wake and SWS. Baseline corrected number of unit activity within 30 ms after stimulation is shown (*$p < 0.05$, **$p < 0.01$ [Ipsilateral: 7 units, contralateral: 4 units, paired t-test]).

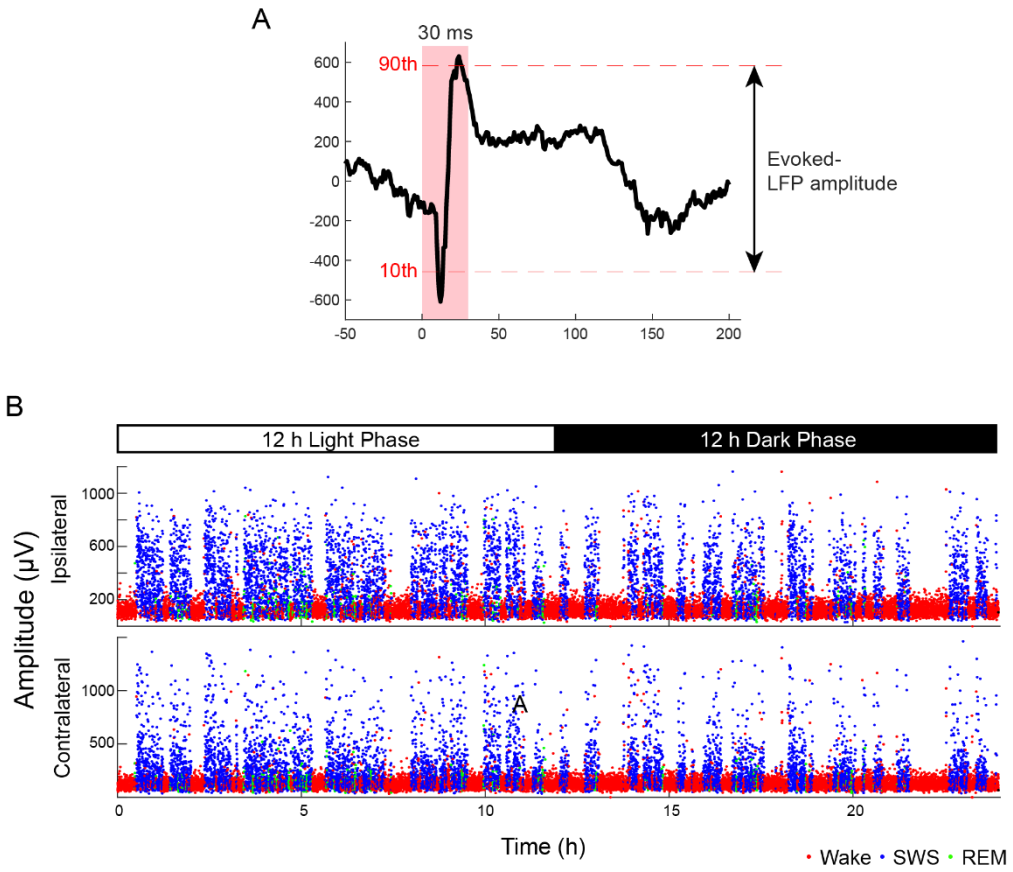

Figure 4. Chronic Optogenetic Probing of Cortical Responses

(A) A representative example of LFP during the light stimulation and the illustration of the measurement process of evoked LFP amplitude. The evoked LFP amplitude was determined from 30 ms time window (red area) after each stimulus onset. The 10th to 90th percentile difference in the distribution of samples (red dash lines) in this time window of each stimulation was used as the evoked LFP amplitude. (B) Representative plot of LFP response amplitude over 24 h from both an ipsilateral and contralateral tetrode in response to unilateral optogenetic stimulation (approximately 17,280 stimuli). Response amplitudes were calculated as the 10th to 90th percentile difference

in LFP signals in a 30-ms time window following stimulation. Plots are color coded: red = wake, blue = SWS, and green = REM sleep.

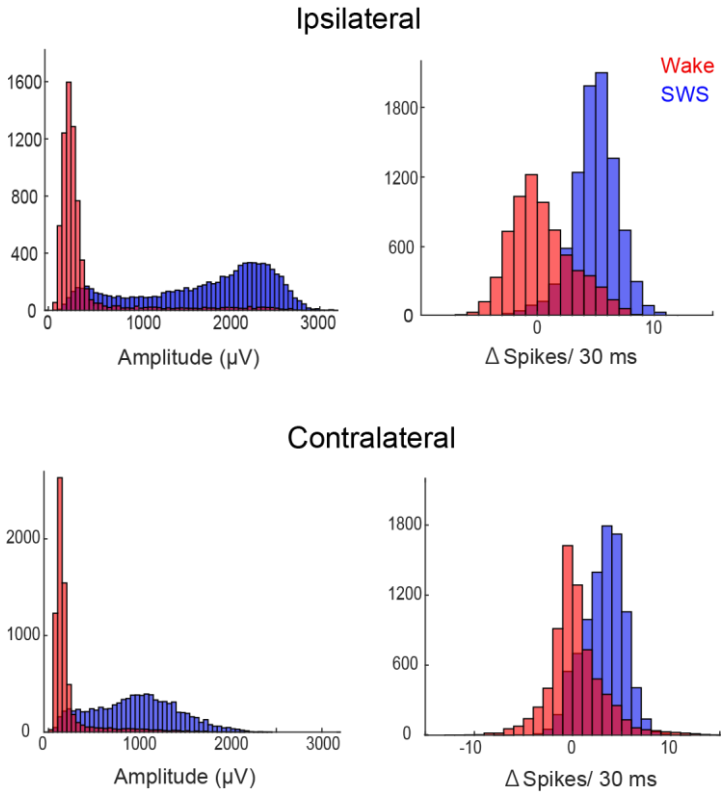

Figure 5. Distribution of Response Amplitudes and MUA in Wake and SWS Histogram of the distribution of LFP response and evoked unit activity in wake and SWS (bin width: 50 μV for LFP, 1 spike for units).

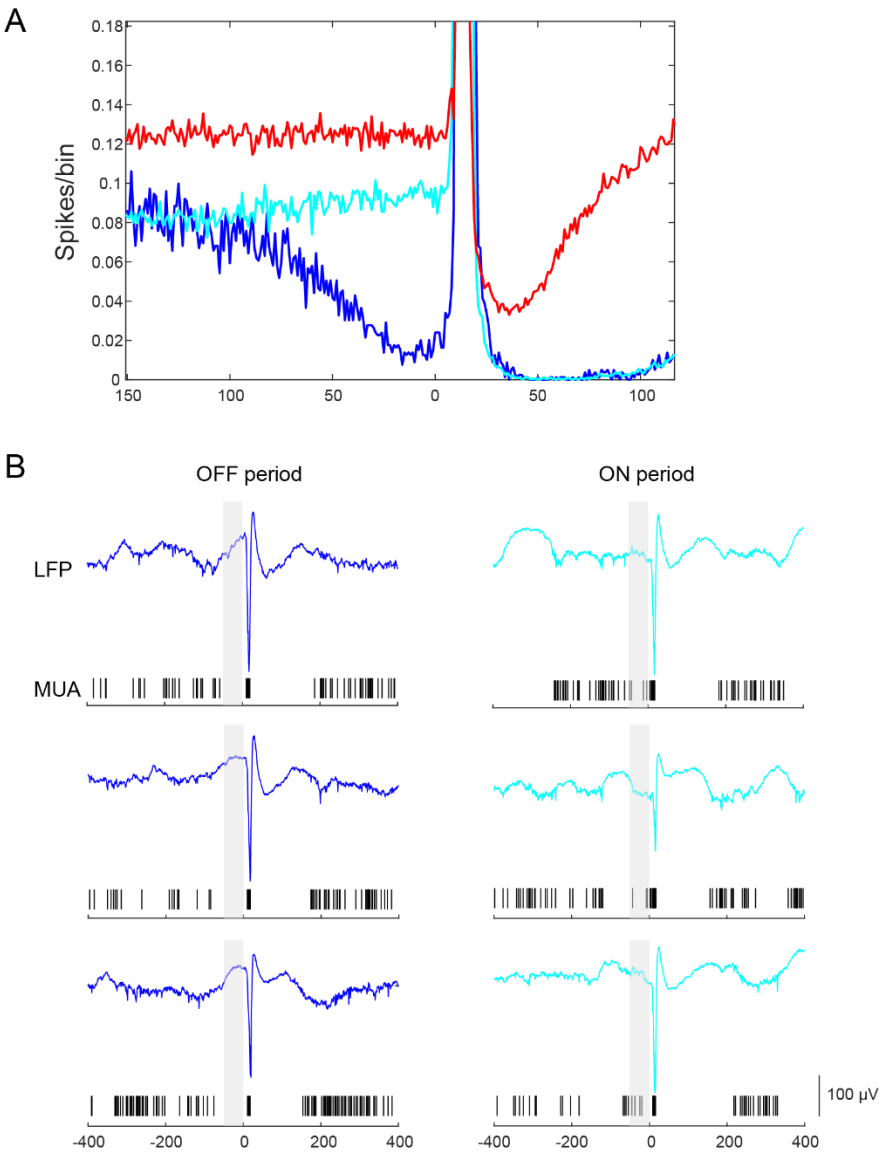

Figure 6. LFP-based ON/OFF period detection

(A) High resolution of the MUA histogram (1 ms bin) with the light stimulation time point at 0 (red: wake, dark blue: OFF period, light blue: ON period). Note the low unit activity level in the OFF stimulation trace just before stimulation. (B) 3 example traces which were categorized as OFF (dark blue, left) or ON (light blue, right) at the time of stimulation. Note the characteristic upward deflection

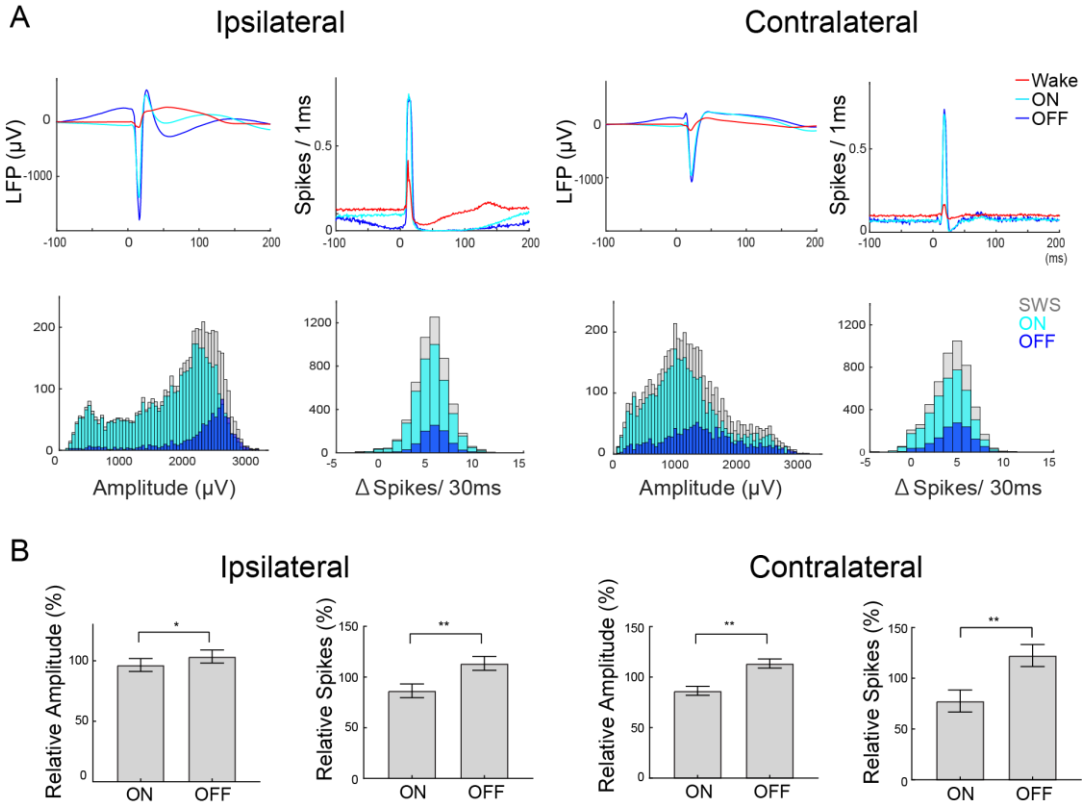

Figure 7. Response Dynamics Across ON/OFF Period of SWS Slow Oscillation

(A) Example traces of mean LFP and MUA responses during wake, SWS-ON, and SWS-OFF period (red: wake, light blue: ON, dark blue: OFF, top) and the distribution of LFP and MUA responses (light blue: ON, dark blue: OFF, gray: all SWS, bottom). Stimuli were delivered every 5 ± 1 s and post-hoc separated into ON and OFF period (see Materials and Methods) depending on LFP and MUA immediately preceding the stimulus for each tetrode. (B) Summary of the difference of the response during ON/OFF period (mean of the medians in each tetrode for LFP amplitude and mean for MUA were normalized to the arithmetic mean of ON and OFF response, error bar: SD, *$p < 0.05$, **$p < 0.01$ [N = 4, paired t-test]).

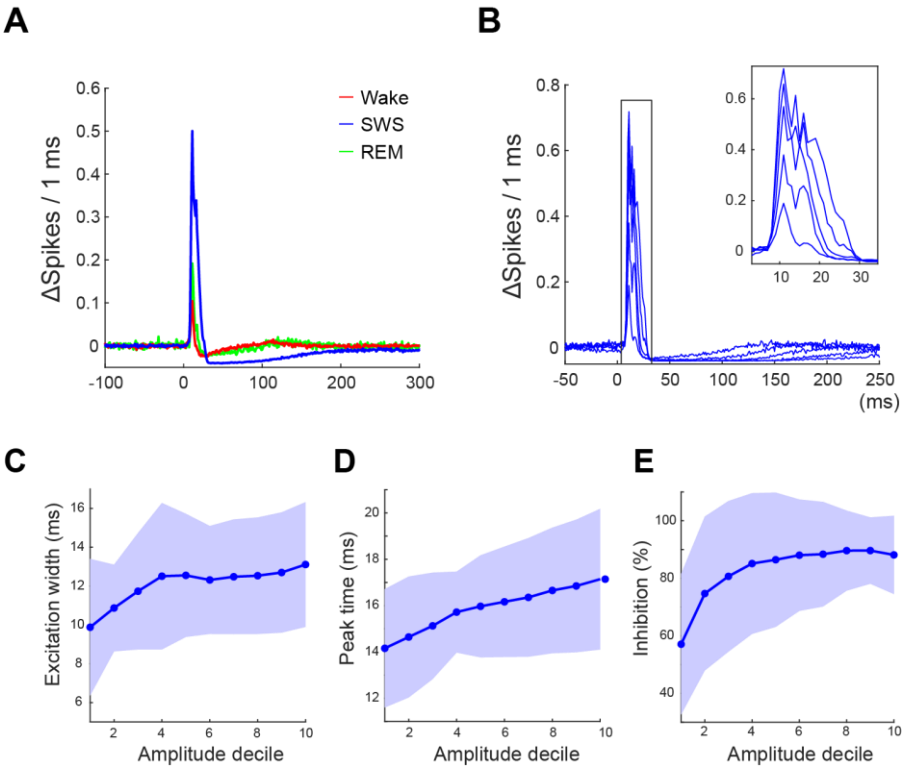

Figure 8. Reduced Feedforward Inhibition in Larger Responses

(A) Peri-stimulus time histograms (1 ms bin size) of MUA in each state. (B) Histograms of quintile of SWS MUA response. (C–E) Development of the action potential firing time-course as a function of the response amplitude (in deciles). (C) Excitation width of the response, defined as full-width at half-maximum of the excitation peak in the histogram (Mean ± SD). (D) The response peak time, defined as the bin with the largest number of action potentials. (E) The percentage of inhibition defined as the % of the reduction of number of unit activity from 50 to 100 ms after stimulation to the number of unit activity of the time window from 150 to 50 ms before the stimulation.

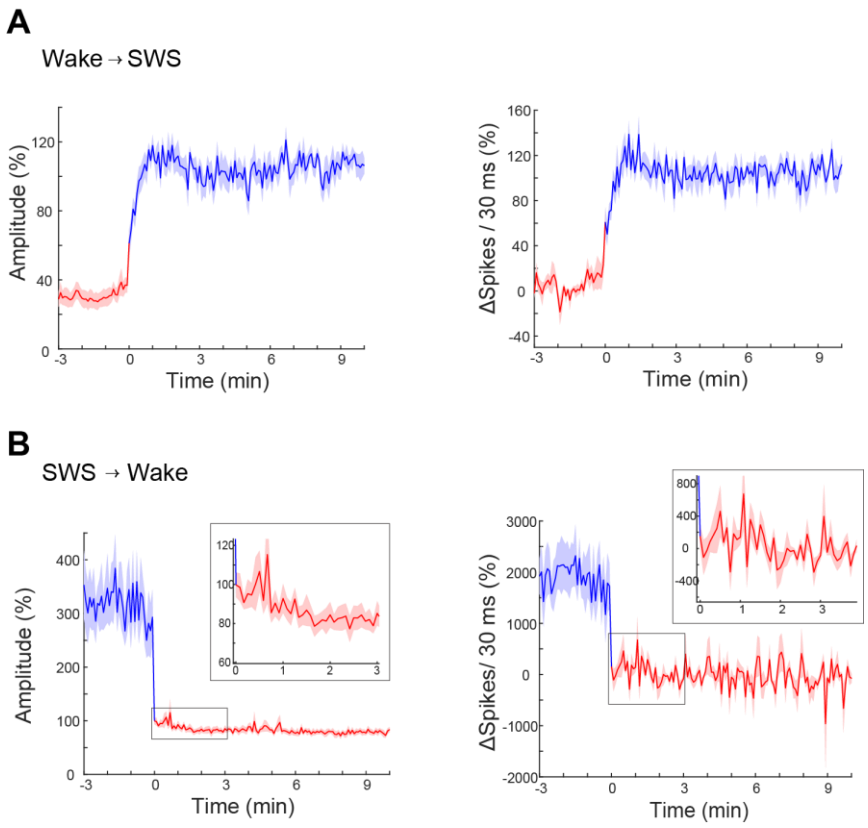

Figure 9. Fast Transition Kinetics of LFP- and MUA- Response Size at Vigilance State Change.

Plot of mean LFP and MUA response as a function of time since beginning of the episode. SWS or wake episodes longer than 10 min that occurred after longer than 3 min wake or SWS episodes were selected. LFP and MUA responses were aligned at their transition and LFP-response amplitudes and the MUA response were averaged after normalizing to the whole 13 min mean of each recording (115 wake to SWS and 76 SWS to wake transition from 4 animals, mean ± standard error of the mean (sem)). (A) Changes in the cortical response following state transitions took less than a minute in either direction, with the transition from SWS to wake taking the least amount of

time. Within SWS cortical responses were highest 30–50 s after detection of the wake-SWS transition. After this peak, the responses slowly decayed by 10–20% over 3 min. (B) SWS to wake transitions were faster and showed little adaptation of the response during the subsequent wake episode by 10–20% over 1–2 min.

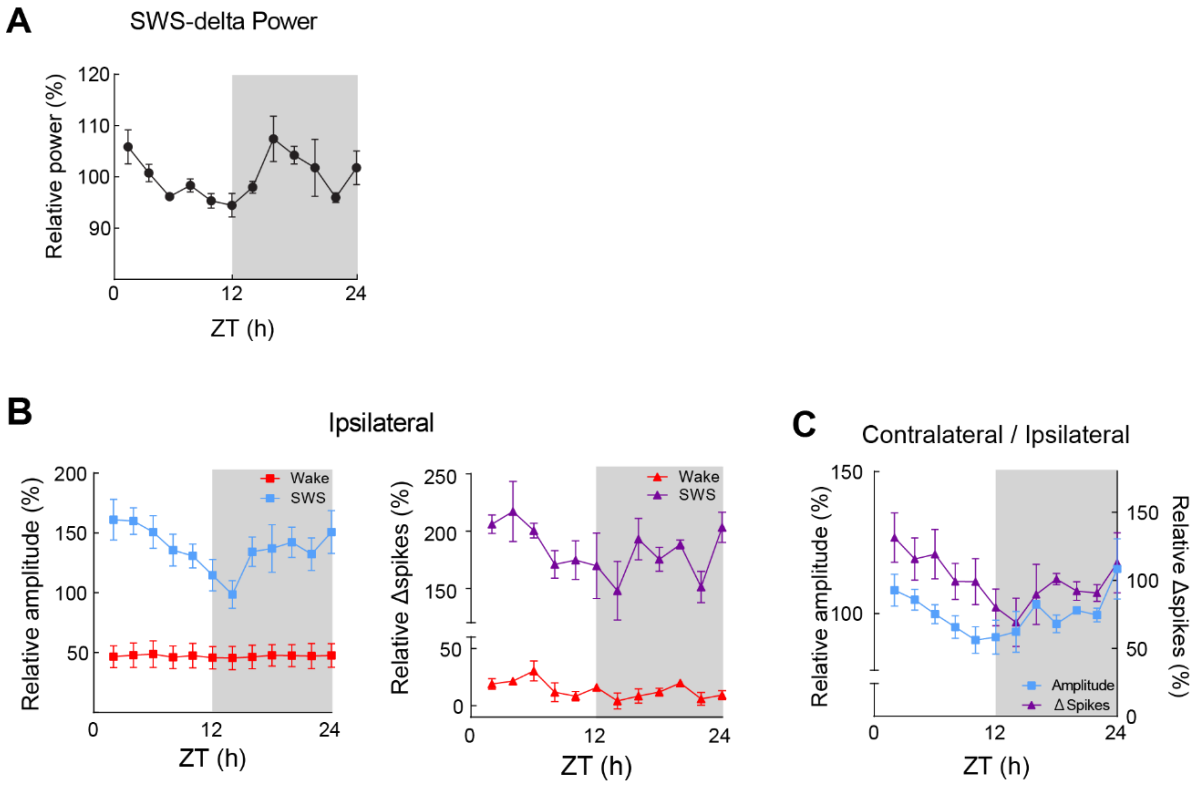

Figure 10. Daily Fluctuation on LFP and MUA Response in SWS but Not in Wake

(A) Dynamics of delta power over 24 h recording. (B) LFP (left) and MUA (right) responses in SWS (blue) and wake (red) over 24 h. Medians of the measurements over 2 h are expressed as percentage of the 24 h mean (error bar: sem). Note the dynamics correlated to light-dark cycle; decreasing during the light phase and increasing during dark phase for both LFP response amplitude and unit response (LFP amplitude: $p < 0.05$, Spikes: $p < 0.05$, [8 recordings, repeated measurement ANOVA]). (C) Contralateral response size divided by the ipsilateral response size over 24 h as intracortical response.

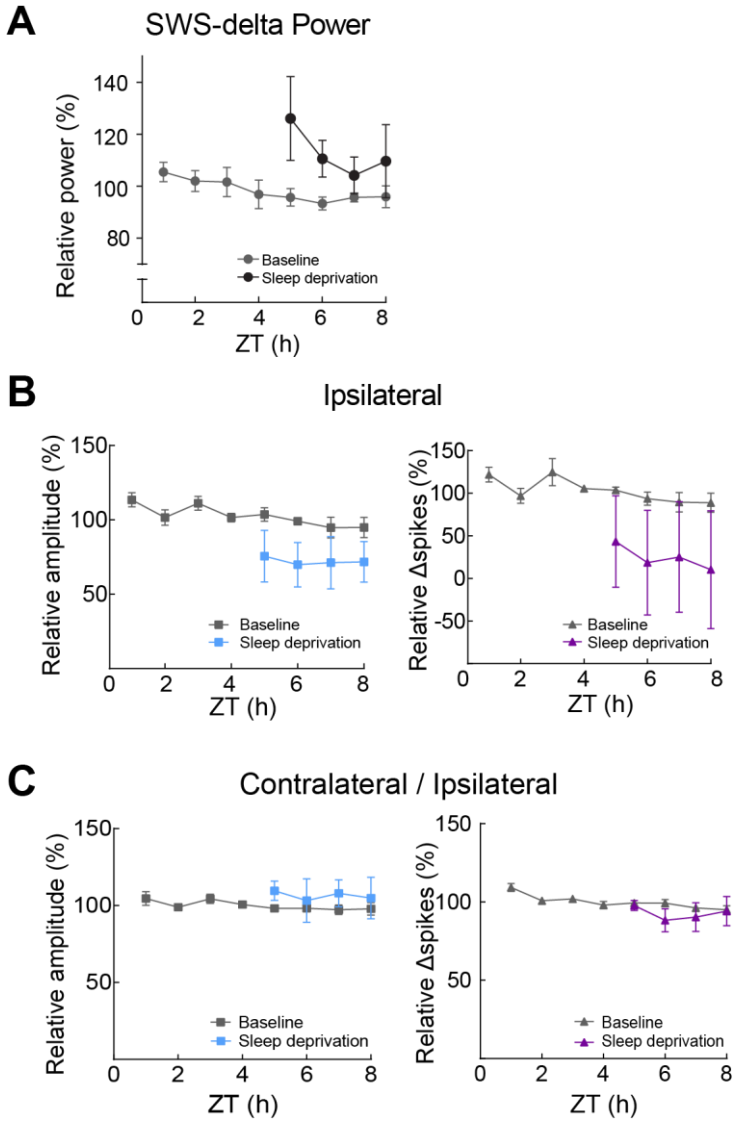

Figure 11. Cortical Responsiveness During Recovery Sleep after Sleep Deprivation

(A) Delta power was averaged over 1 h windows and plotted against Zeitgeber time (ZT) during recovery sleep after 4 h sleep deprivation starts at ZT = 0 ($p < 0.01$, [6 recordings, paired t-test in first hour of recovery sleep]). Gray traces show baseline behavior. (B) LFP (left) and MUA (right) response size for 4 h during recovery sleep is plotted against ZT (mean of the medians over

1 h bin in each tetrode for LFP amplitude and mean over 1 h bin for MUA were normalized relative to the mean of baseline, error bar: sem, LFP amplitude: p = 0.14, Spikes: p = 0.30, [6 recordings, paired t-test in first hour of recovery sleep]). (C) LFP (left) and MUA (right) of intracortical response after for 4 h during recovery sleep relative to the mean of baseline plotted against ZT (error bar: sem, LFP amplitude: p = 0.24, Spikes: p = 0.45 [3 recordings, paired t-test in first hour of recovery sleep]).

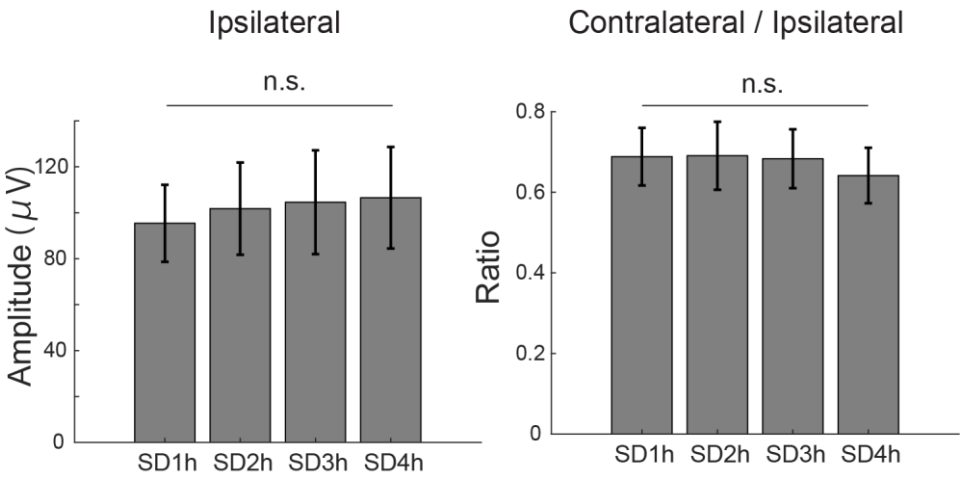

Figure 12. Cortical Responsiveness During Sleep Deprivation

Average of the median LFP responses in wake during sleep deprivation error bars show SD. (3 recordings, repeated measurement ANOVA).

ZT 0 (09:00-) ZT12 (21:00-) ZT 23 (08:00-)

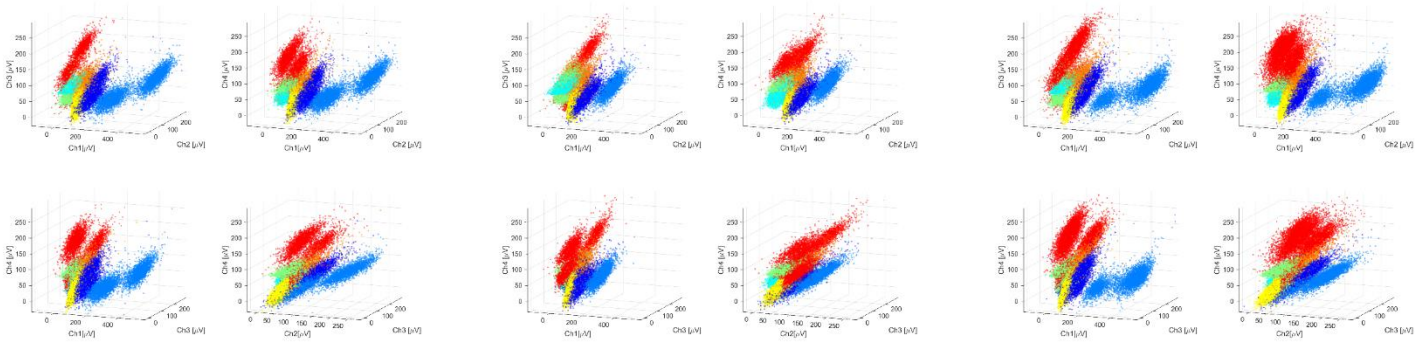

Figure 13. MoDT Spike Sorting of Long-Term Tetrode Recording Data

An example tetrode clustering result. Tetrode has 4 channels and the peak amplitude 3D scatters of 4 possible channel combination colored by the clustering results from the beginning of recording (left), in the middle (middle) and the last (right) 20 min are shown.

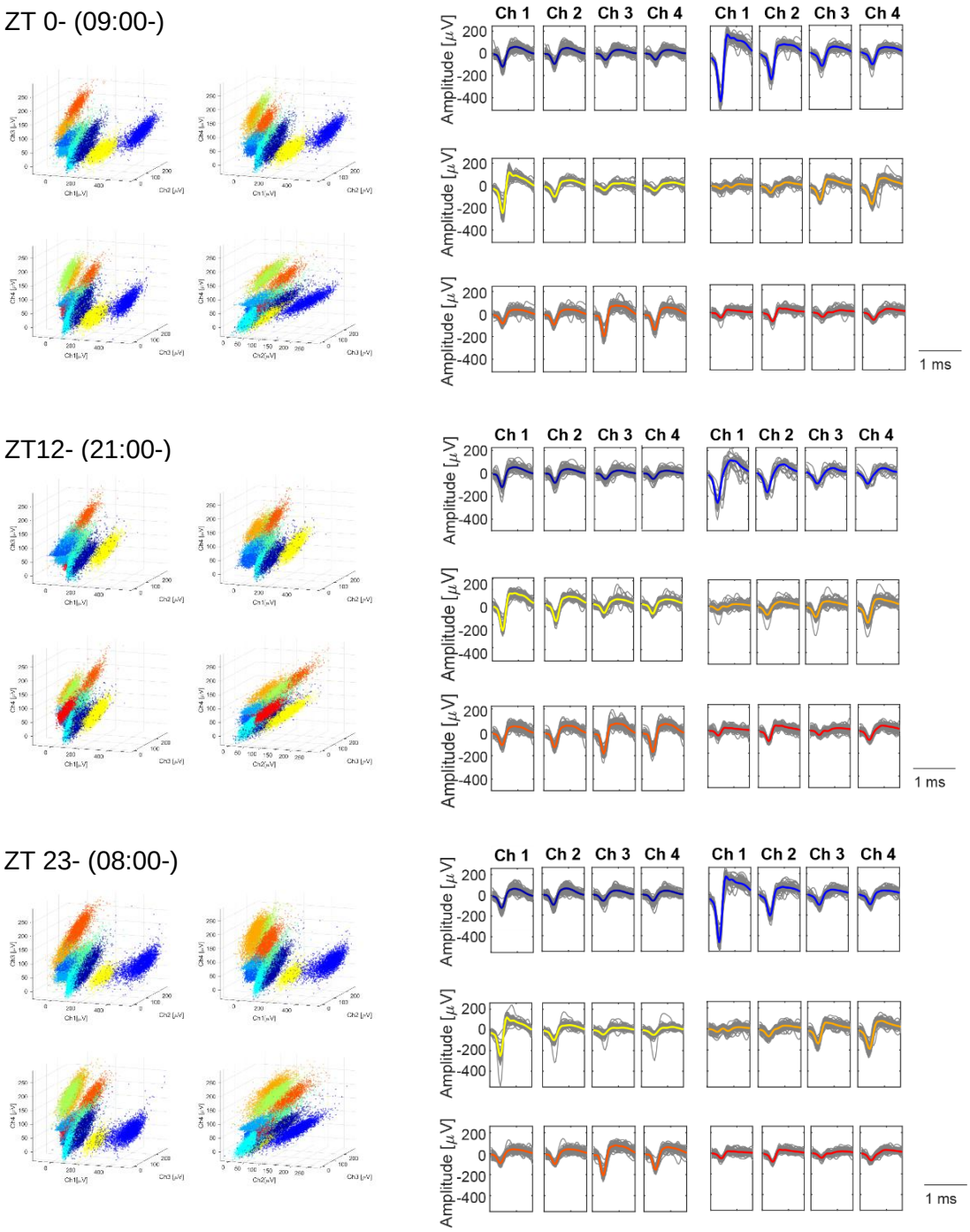

Figure 14. Clusters after Repeated Spike Sorting

The same example tetrode shown in Fig. 13 after hierarchical sorting. The peak amplitude 3D scatters of 4 possible channel combination colored by the clustering results (left) and the wave form of obtained clusters (right) from

the beginning of recording (top), in the middle (middle) and the last (bottom) 20 min are shown.

References